Gas Permeability of Surface-Selectively Chlorinated Poly(4-methyl-1-pentene)

Juha-Matti Levänsalmi and Thomas J. McCarthy*

Polymer Science & Engineering Department, University of Massachusetts, Amherst, Amherst, Massachusetts 01003

Received September 28, 1994; Revised Manuscript Received November 29, 1994[⊗]

ABSTRACT: Heterogeneous (gas−solid) photochlorination reactions of a poly(4-methyl-1-pentene) film were studied with the objective of determining factors that control the surface selectivity of the modification reaction. By adjusting the chlorine vapor pressure, light source intensity, and reaction time, the depth of the chlorination reaction (thickness of the modified layer) and the extent (density) of chlorination (Cl:C ratio) could be independently controlled. Gas permeabilities of asymmetric membranes prepared by this reaction to hydrogen, carbon dioxide, oxygen, and nitrogen were determined. Light chlorination (low Cl:C ratio) at both deep and shallow levels and extensive (Cl:C ~1:1)/shallow chlorination yielded membranes exhibiting no changes in permeability relative to virgin poly(4-methyl-1-pentene). A densely and deeply chlorinated membrane was shown to have improved selectivities over those of unmodified poly(4-methyl-1-pentene). The selectivity increased the most (from 16.5 to 95.9) for H_2/N_2 and the least (from 2.1 to 2.6) for CO_2/O_2, with accompanying decreases in flux.

Introduction

Studies to correlate macroscopic polymer surface properties (adsorption, adhesion, wettability, friction) with surface chemical structure have been underway in our laboratory for several years. We have developed synthetic routes to chemically modified polymer surfaces with the objective of preparing substrates with controllable surface structures so that we can control (and understand) macroscopic surface properties. Much of our effort has been toward controlling the surface selectivity of modification reactions so that thin layers (10−100 Å) of reactive functionality can be introduced to relatively thick film samples. Surface-selective modifications have been reported for polyethylene,[1] poly(chlorotrifluoroethylene),[2−5] poly(vinylidene fluoride),[6] polypropylene,[7] poly(tetrafluoroethylene-*co*-hexafluoropropylene,[8] and poly(ether ether ketone).[9] Under certain conditions[1] the photochlorination of polyethylene was found to be surface-selective. We attribute the surface selectivity to the formation of a barrier layer (chlorinated polyethylene) that inhibits permeation of chlorine to greater depths. Surface-selective modifications of this type (that exhibit autoinhibition and create a less permeable skin) may be useful for the preparation of asymmetric nonporous membranes for gas separation.

Asymmetric membranes, with a bulk region (50−300 μm) exhibiting low selectivity and high permeability and a dense skin region (0.1−0.5 μm) exhibiting high selectivity and low permeability, were developed to meet the requirements of high productivity and high mechanical strength.[10] Membranes of this type have traditionally been prepared by phase inversion or by constructing composite structures. Surface modification of polymer films to introduce a selective surface layer is an alternative approach to asymmetric gas separation membranes. Accurate control of the depth and extent of reaction and control of the chemical nature of the selective layer are needed to optimize the trade-off between selectivity and permeability.

We report here a study of the heterogeneous (gas−solid) chlorination of poly(4-methyl-1-pentene) (PMP). PMP was an attractive choice for several reasons: It has the lowest density of all commercially available thermoplastics and a higher permeability to gases than the other hydrocarbon polymers. It is reasonably temperature and chemical resistant with a softening point of 160−170 °C, melting point of 230−240 °C, and an all-aliphatic structure. As a saturated hydrocarbon it should react with chlorine via an unexceptional photoinitiated chain reaction. Fluorination of PMP membranes has been shown to improve selectivity for certain gas pairs.[11,12] Chlorination is a less exothermic and more easily controlled reaction than fluorination which can cleave C−C bonds resulting in polymer degradation. The instability of fluorinated PMP membranes[13] may be the result of degradation during reaction.

PMP is semicrystalline with a density of 0.813−0.828 g cm^{-3} for crystalline regions and 0.838−0.839 g cm^{-3} for amorphous regions. The glass transition temperature is reported to be 22−30 °C.[14] PMP is unique in having crystalline regions of lower density than amorphous regions. The low density of PMP crystals is explained by inefficient packing of chains in the various crystalline forms. No permeation of gases takes place in the crystalline regions of most semicrystalline polymers, but the solubility of gases with molecular diameters smaller than 4 Å in the PMP crystalline region is about 25−30% of that in the amorphous region.[14]

Experimental Section

General Procedures. PMP film (50 μm Mitsui TPX) was extracted in refluxing dichloromethane for 1 h and dried at reduced pressure and room temperature to constant mass. Chlorine gas (Aldrich: 99.5+%) was used as received. XPS spectra were obtained with a Perkin-Elmer Physical Electronics 5100 spectrometer using Mg Kα excitation (400 W, 15.0 kV). Spectra were routinely recorded at a takeoff angle of 15° (measured between the film surface plane and the entrance lens of the detector optics); 75° takeoff angle data for some samples are reported. Atomic composition data were determined using sensitivity factors obtained from samples of known composition: C_{1s}, 0.225; Cl_{2p}, 0.655. Attenuated total reflectance infrared (ATR IR) spectra were recorded using an IBM 38 FTIR at 4 cm^{-1} resolution with a 10 × 5 × 1 mm KRS-5 internal reflection element (45°). Gravimetric measurements were made with a Sartorius 1612MP8-1 analytical balance. Dynamic advancing (θ_A) and receding (θ_R) contact

[⊗] Abstract published in *Advance ACS Abstracts,* February 1, 1995.

0024-9297/95/2228-1733$09.00/0

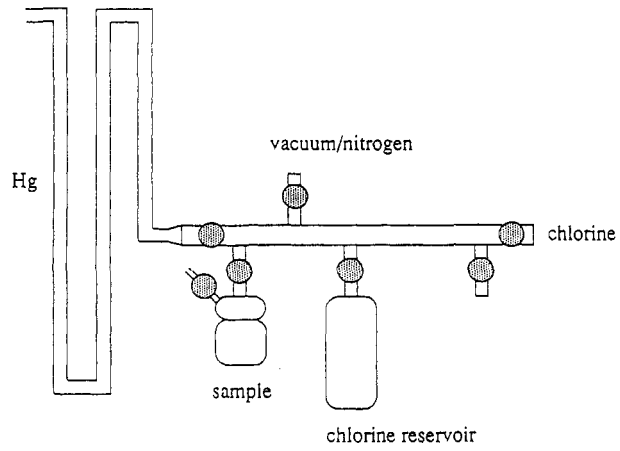

Figure 1. Gas/vacuum manifold used for heterogeneous chlorination reactions.

angles were measured with a Ramé-Hart telescopic goniometer and a Gilmont syringe with a flat-tipped 24-gauge needle as probe fluid was added (θ_A) or withdrawn (θ_R) from the drop. Phase interference microscopy was performed using a Zygo Maxim 3D Model 5700. Surface chlorinations were run on both sides of the film controlling reaction time (15 s to 17 h), chlorine pressure (5 mm to 1 atm—regulating the vapor pressure with cold baths), and light intensity (darkness, ambient hood light, a medium-intensity UV light source (UVP Inc., Model UVG-11) of 330 μW/cm^2 at 254 nm, and a high-intensity UV light source (UVP Inc., Blak-Ray B-100A) of 6000 μW/cm^2 at 365 nm).

Chlorination. A secondary vacuum manifold (Figure 1) that could be evacuated and filled with nitrogen or chlorine was used for the heterogeneous chlorinations of a PMP film. For reactions that were run in the dark, the manifold was wrapped with a thick, black cloth. Reactions were also run in ambient hood light or using a UV light source placed at the base of an aluminum foil funnel below the sample container. The sample vessel (containing the tared sample), chlorine reservoir, and secondary manifold were evacuated, subsequently filled with nitrogen several times, and then evacuated. The sample container was isolated from the rest of the manifold, and chlorine gas (5 psig) was introduced. Cold baths were used to adjust the chlorine vapor pressure by placing the bath around the chlorine reservoir. The vapor pressure in the closed system was allowed to equilibrate, and the reaction was started by opening the sample container valve after closing the chlorine reservoir valve. The reaction manifold/sample container was calibrated (with a manometer) to have reaction pressures of 176, 47, 16, and 5 mm using temperature baths of −44, −63, −83, and −97 °C, respectively. For reactions run at 1 atm of chlorine pressure, the manifold was depressurized (from a slight overpressure) through a bubbler to let pressure equilibrate with the outside pressure. The reaction was stopped by evacuating the system and replacing the unreacted chlorine and product HCl with nitrogen. Film samples were dried/degassed to constant mass and stored under nitrogen prior to additional analyses.

Gas Permeation Rate Measurements. Gas permeation studies were run one gas at a time with hydrogen, carbon dioxide, oxygen, and nitrogen at 40 °C with an upstream pressure of 6 atm (3.5 atm for H_2) and a downstream pressure of 0 atm. After reaching a steady-state flux of gas, a pressure increase of 0.50 mm in a known volume on the downstream side was timed. A home-built pressure/vacuum manifold was built around a Millipore 25 mm membrane cartridge (25 mm diameter) and a Celesco DP 31 differential pressure transducer.

Results and Discussion

Exposure of PMP film samples to Cl_2 gas at room temperature and ambient light conditions induces a rapid and extensive radical chain chlorination as evi-

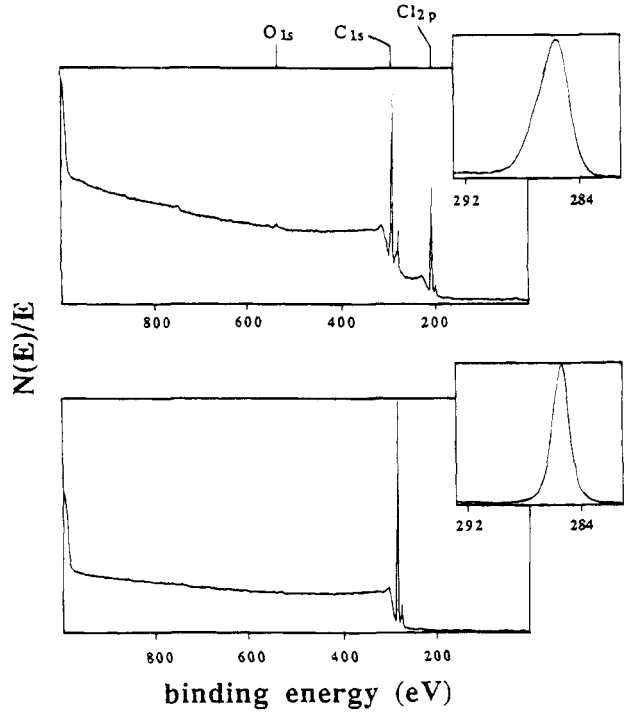

Figure 2. Survey and C_{1s} region XPS spectra for virgin PMP (lower spectra) and a PMP sample that was chlorinated at 1 atm of Cl_2 pressure at ambient light conditions for 1 min (upper spectra).

denced by X-ray photoelectron spectroscopy (XPS) and gravimetric analysis. Figure 2 shows XPS survey and C_{1s} region spectra for a virgin PMP film sample and a sample that had been exposed to 1 atm of Cl_2 for 1 min. This sample increased in mass by 2.4%. The XPS spectra were recorded at a 75° takeoff angle, which assesses the composition of the outer ~40 Å of the film. The composition of this region is $C_{100}Cl_{23}$ (~1.4 Cl per PMP repeat unit) which corresponds to 37 wt % chlorine. The broadened C_{1s} spectrum indicates that C−Cl (carbon bound to one chlorine) is present in this sample. C−Cl and CCl_2 (carbon bound to two chlorines) are important structural features of chlorinated PMP (see below). Variable small amounts of oxygen are observed in product films (seen in Figure 2); we attribute this to termination of the radical chain reaction by adventitious oxygen. PMP contains primary, secondary, and tertiary C−H bonds, so a range of chlorinated product structures are possible; we do not attempt in this paper to distinguish among them but regard the reaction as a simple replacement of hydrogen atoms with Cl atoms. Other aspects of the reaction are inherently complex. The kinetics and surface selectivity (relative rates of reactions at different depths) will depend on both Cl_2 concentration and photointensity in ways not easily predicted. High Cl_2 concentration and high photointensity should yield rapid conversion, but the product may inhibit further reaction by acting as a barrier layer for Cl_2 diffusion.

A series of heterogeneous photochlorinations of a PMP film were carried out using a vacuum/gas manifold as a reactor with which reaction time, chlorine pressure, and photointensity could be conveniently controlled (see Figure 1). The reaction time was varied from 15 s to 17 h by opening a valve to start the reaction and evacuating the manifold to stop the reaction. Chlorine pressure was varied from 5 mm to 1 atm using low-temperature baths to control subatmospheric pressures. Photointensity was controlled to four reproducible con-

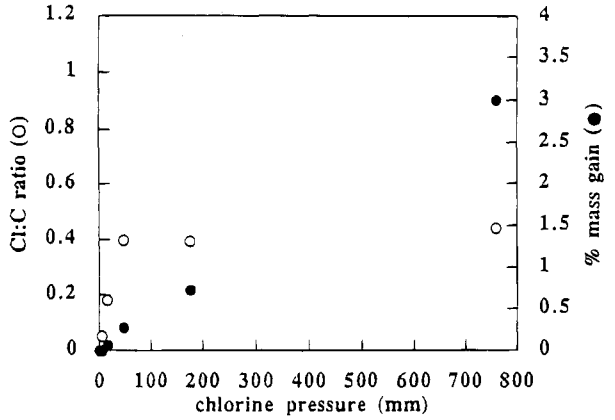

Figure 3. XPS and gravimetric data for PMP samples chlorinated in ambient light for 2 min.

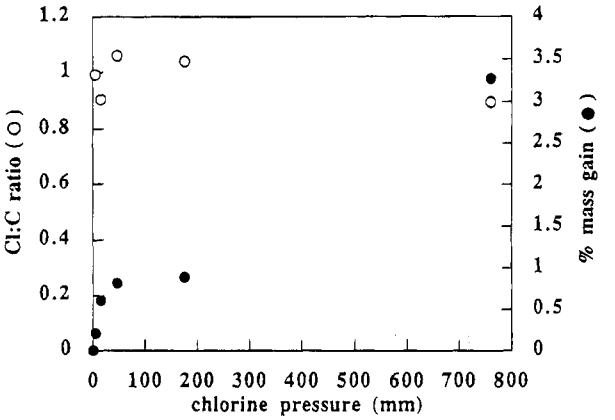

Figure 4. XPS and gravimetric data for PMP samples chlorinated in high-intensity UV light for 2 min.

ditions by wrapping the reactor with a black cloth ("dark"), exposing the reactor to ambient hood light, or shining either a medium- or high-intensity UV light source on the sample container. The effects of these three variables on both the depth of reaction and the density (on the PMP chain) of chlorination were studied with the objective of establishing conditions with which reproducible and independent control over both chlorination depth and chain density could be exercised. Gravimetric analysis and X-ray photoelectron spectroscopy (XPS) were used as survey analytical methods. XPS yields a precise determination of atomic composition from which Cl:C ratios and chlorination densities can be determined for the outermost 10–40 Å of the film samples. Gravimetric analysis yields the total chlorine content of the film samples from which (along with XPS data) depths of reaction can be estimated. Conditions were then chosen to prepare four prototypical membranes: a deeply and highly chlorinated sample **(H&D)**, a deeply and lightly chlorinated sample **(L&D)**, a shallowly and highly chlorinated sample **(H&S)**, and a shallowly and lightly chlorinated sample **(L&S)**. These prototypes were analyzed in more detail with regard to structure, composition, and their potential as gas separation membranes.

Effect of Chlorine Pressure. The rate of diffusion of chlorine into a PMP film is controlled by the chlorine vapor pressure. The effect of chlorine pressure on the product structure was studied under reaction conditions of ambient, medium-intensity UV, and high-intensity UV light and over a range of reaction times. Representative data that summarize pressure effects are presented here.

Figure 3 shows plots of both mass increase and Cl:C ratio (determined by XPS at a takeoff angle of 15°—indicative of the composition of the outermost 10 Å) versus chlorine pressure for PMP samples chlorinated for 2 min under ambient light conditions. Figure 4 shows the same data for PMP samples chlorinated for 2 min under high-intensity UV conditions. At Cl_2 pressures above 50 mm for ambient light conditions and at all pressures studied under UV light, the extent of chlorination (density of chlorine atoms on the chain) is independent of pressure. Chlorine:carbon ratios of ~0.4 and ~1 are obtained for ambient and high-intensity UV light conditions, respectively, indicating compositions of $C_{100}Cl_{\sim 40}$ (51 wt % chlorine—2.4 Cl atoms per PMP repeat unit) and $C_{100}Cl_{\sim 100}$ (73 wt % chlorine—6 Cl atoms per PMP repeat unit). The mass increases, however, are highly dependent on chlorine pressure. A linear dependence on pressure is observed for the 2 min reactions under ambient light conditions (Figure 3). A PMP sample increased in mass by 0.6% at 16 mm, and at 760 mm a 3% mass gain was observed. A 47.5-fold difference in pressure yielded a 50-fold difference in mass gain. This indicates an approximate first-order rate dependence on chlorine concentration and also that mass uptake can be controlled over a significant range using pressure control. Under UV light conditions, the effect of chlorine pressure on mass increase (Figure 4) is not linear, and a greater pressure dependence is observed at low pressures. At 5 and 16 mm, mass increases of 0.2% and 0.6% were observed, indicating an approximate first-order chlorine dependence, but at 760 mm a 3.3% mass gain occured—a 5-fold increase with a 47.5-fold pressure difference over the reaction at 16 mm. Nonlinear pressure dependences of this type were observed for all reactions that produced samples that had XPS Cl:C ratios greater than ~0.6. This suggests samples containing a sufficiently high chlorine content in their modified surface region exhibit barrier properties to chlorine gas.

The dependence of mass uptake and the independence of XPS the Cl:C ratio on chlorine vapor pressure allow control of the thickness of the modified layer at a constant chlorine content.

Effect of Light Source Intensity. The photointensity controls the rate of formation of chlorine radicals that initiate radical chain chlorination and thus the concentration of radical specis in the PMP film region that chlorine has diffused to during reaction. The higher the photointensity, the higher the probability that chlorine molecules that diffuse into the film will react with PMP chain radicals rather than diffuse deeper into the film sample. Figure 5 indicates that photointensity controls the composition (Cl:C ratio) of the XPS sampling region. Chlorine:carbon ratios are plotted versus reaction time for samples prepared at 1 atm of Cl_2 under the four light conditions studied. The plots indicate that for the ambient and UV conditions most of the reaction in the XPS sampling depth occurs in the first 2–5 min. Compositions level at Cl:C = ~0.6, ~0.8, and ~1.1 for ambient, medium-intensity UV, and high-intensity UV light, respectively. Reaction in the XPS sampling depth for the dark chlorination is slower and has not leveled at the times shown in Figure 5. Samples chlorinated for 40 and 120 min exhibited Cl:C ratios of 0.1.

Figure 6 exhibits gravimetric data for the samples described in Figure 5. Samples continue to gain mass with longer reaction times under all photointensity conditions, indicating that good barrier properties to-

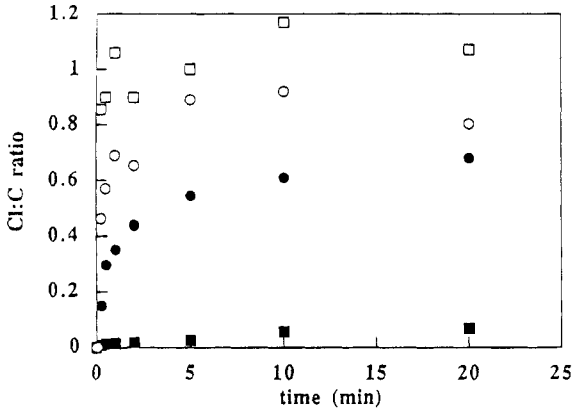

Figure 5. XPS data for PMP samples chlorinated at 1 atm of Cl_2 pressure in the dark (■), in ambient light (●), in medium-intensity UV light (○), and in high-intensity UV light (□).

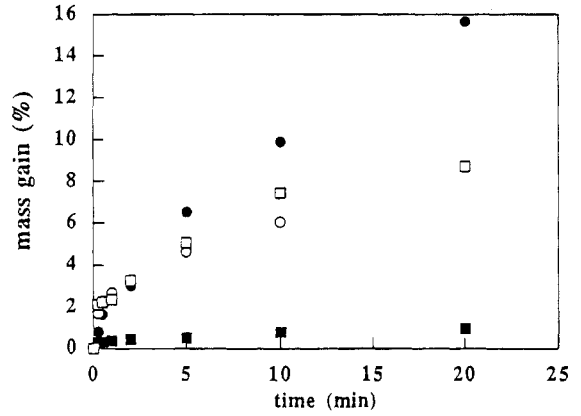

Figure 6. Gravimetric data for PMP samples chlorinated at 1 atm of Cl_2 pressure in the dark (■), in ambient light (●), in medium-intensity UV light (○), and in high-intensity UV light (□).

ward chlorine are not achieved under any conditions: reactions proceed deep into the bulk of the film. The differences in mass uptake rate between the ambient, medium-intensity, and high-intensity light conditions indicate that barrier properties are improved with increasing photointensity. The mass increases that occurred between 10 and 20 min of the photochlorination reactions were 5.8%, 2.6%, and 1.3% for ambient, medium-intensity UV, and high-intensity UV conditions, respectively. The inverse dependence of rate on photointensity can only be explained by a diffusion rate that decreases with photointensity. The XPS composition data are consistent with this observation; the more highly chlorinated surfaces function as better barrier layers (compare Figures 5 and 6).

Effect of Reaction Time. Summary of Variable Effects. The data in Figure 5 indicate that, after rather short reaction times, the extent of chlorination in the XPS sampling region is independent of reaction time. This was found to be true, in general, for chlorination reactions at all Cl_2 vapor pressures under all light conditions studied. Controlling chlorination extents with reaction time is thus not practical and, in practice, is more easily accomplished by controlling photointensity. The mass, however, increases regularly with reaction time as indicated by the plots in Figure 6. Reaction time is thus a variable that is as useful as Cl_2 vapor pressure in controlling mass gain or thickness of the modified layer. We have concluded that the most convenient means of preparing modified PMP samples of desired extents and depths of chlorination is to use an appropriate chlorine pressure and light source and fine-tune the modification by adjusting the reaction time.

Determining reaction depths or thicknesses of chlorinated layers is not straightforward. Thickness values can be calculated from the XPS composition and gravimetric data, but the values are meaningful only relatively. If we assume that the composition of the modified layer is that indicated by the XPS data, then the stoichiometry of the reactions can be determined. For example, the samples chlorinated at different pressures in ambient light for 2 min (Figure 3) have Cl:C ratios of 0.1 (5 mm), 0.18 (16 mm), 0.40 (47 mm), 0.40 (176 mm), and 0.44 (760 mm). These ratios correspond to compositions of $C_{100}H_{190}Cl_{10}$, $C_{100}H_{182}Cl_{18}$, $C_{100}H_{160}Cl_{40}$, $C_{100}H_{160}Cl_{40}$, and $C_{100}H_{156}Cl_{44}$, for the 5, 16, 47, 176, and 760 mm reaction products, respectively. Using estimates of densities for the modified layers (determined from the Cl:C ratio and the densities of PMP and poly(vinyl chloride), thicknesses can be calculated that account for the mass increases observed. Thicknesses of 0.06 (16 mm), 0.13 (47 mm), 0.34 (176 mm), and 1.3 μm (760 mm) are calculated. No mass gain was observed for the sample reacted at 5 mm. These thickness estimates are minima and assume a constant chlorine concentration throughout the modified layer. There is most certainly a gradient structure (see below) with less chlorine at greater depths; thus, the true thicknesses are greater than these estimates.

Chlorine vapor pressure and reaction time thus control the depth of modification, and these depths scale with the mass increases (at constant Cl:C ratios). The photointensity also controls thickness by controlling barrier efficiency. For example, the 20 min reactions at 1 atm of Cl_2 (Figures 5 and 6) give samples with structures of $C_{100}H_{93}Cl_{107}$ (high-intensity UV), $C_{100}H_{120}Cl_{80}$ (medium-intensity UV), $C_{100}H_{132}Cl_{68}$ (ambient), and $C_{100}H_{193}Cl_7$ (dark). Thicknesses of the type discussed above for these samples are 1.5 (high-intensity UV), 2.0 (medium-intensity UV), 4.3 (ambient), and 2.6 μm (dark).

Prototype Membranes. The preliminary chlorination experiments described above indicate that the depth and extent of reaction can be controlled by adjusting three parameters: reaction time, chlorine vapor pressure, and light source intensity. Four modified sample types were chosen for more detailed surface analysis and gas permeation studies; conditions for their preparation were chosen from the preliminary chlorination data. A highly (high Cl:C ratio) and deeply chlorinated membrane **(H&D)** was prepared using high-intensity UV light conditions, 1 atm of chlorine pressure, and a 20 min reaction time. A highly and shallowly chlorinated membrane **(H&S)** was prepared using high-intensity UV light conditions, 16 mm chlorine pressure, and a 2 min reaction time. A lightly (low Cl:C ratio) and deeply chlorinated membrane **(L&D)** was prepared using 1 atm of chlorine pressure, a 120 min reaction time, and dark conditions. A lightly and shallowly chlorinated membrane **(L&S)** was prepared using ambient light, 5 mm chlorine pressure, and a 2 min reaction time.

XPS and gravimetric data for the prototype membranes are summarized in Table 1. Each of the data points is the average of four experimental values. Separate XPS samples were used to obtain 15° and 75° takeoff angle spectra to minimize errors in atomic composition data due to beam damage. Figure 7 shows

Table 1. XPS and Gravimetric Data

sample	Cl:C (15°)[a]	Cl:C (75°)[a]	mass gain (%)
H&D	1.1	1.0	8.4
H&S	0.9	0.8	0.4
L&D	0.05	0.04	2.0
L&S	0.1	0.07	0.0

[a] XPS takeoff angle.

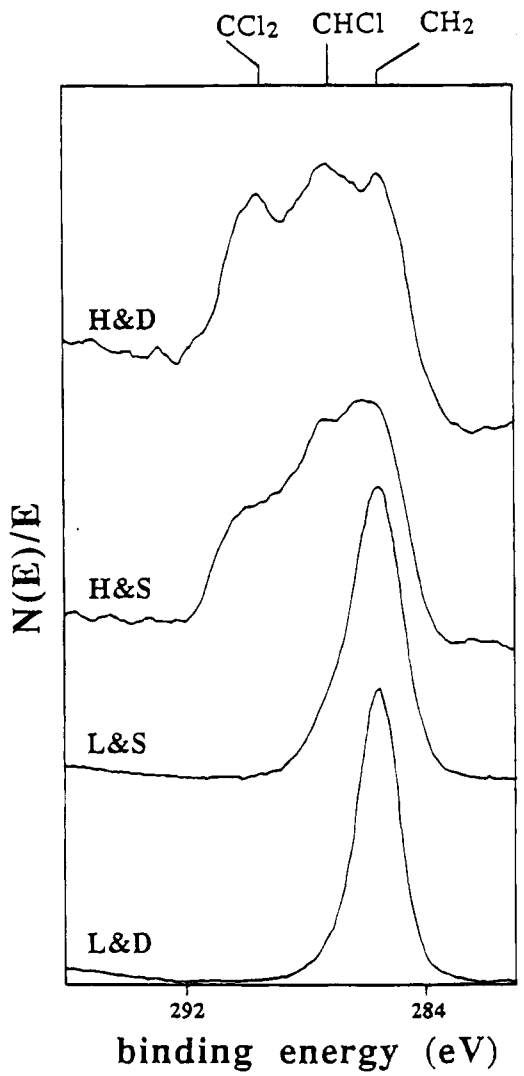

Figure 7. C_{1s} region XPS spectra for the prototype membrane samples.

Table 2. Contact Angle Data

sample	H_2O θ_A	H_2O θ_R	CH_2I_2 θ_A	CH_2I_2 θ_R
PMP	122	95	77	38
H&D	93	65	25	0
H&S	94	64	15	0
L&D	108	68	60	14
L&S	93	68	47	2

XPS C_{1s} region spectra for the four samples: spectra of the highly modified samples show the presence of significant levels of both monochlorinated and dichlorinated carbon species; spectra of the lightly chlorinated samples indicate only light monochlorination. Chlorinated layer thickness values (estimated by the method described above) are 1.5 μm for **H&D**, 0.07 μm for **H&S**, and 4.1 μm for **L&D**. The **L&S** sample gained no measurable mass. The takeoff angle dependence of the

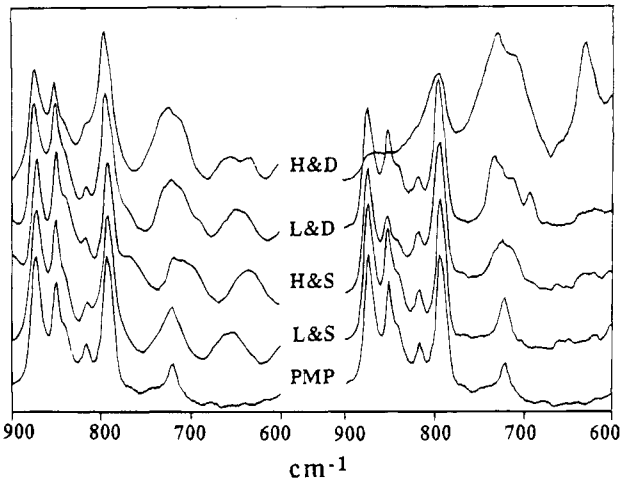

Figure 8. Transmission (left) and ATR (right) infrared spectra for virgin PMP and the prototype membrane samples.

Cl:C ratio, which is observed for all the samples, reveals that the outermost 10 Å of the membranes is more extensively chlorinated than the next deeper 30 Å. This suggests that there is a gradient chlorine density throughout the modified layers of each of the samples and that the calculations underestimate the actual thicknesses. The sharp takeoff angle dependence of the Cl:C ratio for the **L&S** sample (Table 1) and the gravimetric data (no mass gain) indicate a very shallow modification.

The four samples were also analyzed by contact angle analysis, ATR IR, and transmission IR, and an **H&D** sample was analyzed by phase measurement interference microscopy (PMIM). PMIM indicates that no gross topographical changes occur upon chlorination. Contact angle measurements (Table 2) were carried out with both water and diiodomethane as probe fluids. Water contact angles do not clearly differentiate between chlorinated samples, but both advancing and receding angles show clear differences compared with an unmodified film. Measurements with diiodomethane as the probe fluid also show differences within the series of modified samples. Diiodomethane contact angles (that indicate structure in the outermost few angstroms) decrease with increasing chlorine content, as determined by XPS analysis (of a thicker region).

Figure 8 displays transmission and ATR infrared spectra for virgin PMP and the four prototype membranes. C–Cl stretching vibrations are observed at ~740–700 and ~660–620 cm^{-1} for all the chlorinated samples and are more intense with increasing depth and extent of modification. The ATR IR sampling depth under the conditions of these analyses is ~2 μm. Comparing the transmission and ATR spectra of the **H&D** sample reveals that little if any unreacted PMP remains in the ATR IR sampling depth. This suggests that both amorphous and crystalline PMP are chlorinated under these conditions. The transmission spectrum indicates, however, that the majority of PMP in the bulk of the sample is unreacted.

Gas Permeation Results. Gas permeability data (Table 3) shows that, for the set of gases studied, a high extent of reaction in a deeply modified layer is necessary to change diffusion rates and selectivities. The **L&S**, **L&D**, and **H&S** samples exhibit no differences in permeability compared with virgin PMP. The **H&D** chlorinated membrane shows decreased permeabilities for all gases studied. The selectivities between all gas pairs are enhanced in the **H&D** chlorinated membrane

Table 3. Gas Permeability Data

sample	$P(N_2)^a$	$P(O_2)^a$	$P(CO_2)^a$	$P(H_2)^a$
PMP	1.3	5.4	11.5	22.0
H&D	0.12	0.90	2.3	11.8
H&S	1.3	4.5	11.9	20.5
L&D	1.3	4.4	10.7	18.2
L&S	1.1	4.0	11.7	21.1

[a] 10^{-9} cm^3 (STP) cm/cm^2 s·cmHg.

Table 4. Gas Selectivity Data

sample	O_2/N_2	H_2/N_2	CO_2/N_2	CO_2/O_2	H_2/O_2	H_2/CO_2
PMP	4.1	16.5	8.6	2.1	4.1	1.9
H&D	7.3	95.9	18.9	2.6	13.1	5.1

over virgin PMP (Table 4). The largest increase in selectivity is 5.8-fold for the hydrogen/nitrogen pair with a 46% decrease in hydrogen flux. The need for deep modification suggests that a chlorinated layer of PMP does not have excellent barrier properties; the selective skin on typical asymmetric membranes is 0.1−0.5 μm.

Conclusions

The heterogeneous chlorination of poly(4-methyl-1-pentene) can be controlled by choosing the appropriate combination of chlorine vapor pressure, light intensity, and reaction time. The depth of the reaction can be controlled with the vapor pressure and/or reaction time, and photointensity plays an important role in the extent of reaction. Gas permeability data as well as the chlorination kinetics indicate that the chlorinated layer does not have excellent barrier properties. Only highly and deeply chlorinated membranes show decreases in gas permeability. The improved selectivities observed demonstrate that rationally controlled surface modification is a viable route to asymmetric gas separation membranes.

Acknowledgment. Financial support from the Office of Naval Research and the University of Massachusetts CUMIRP program is acknowledged. J.-M. L. thanks the Neste Corporation Foundation for fellowship support.

References and Notes

(1) Cross, E. M.; McCarthy, T. J. *Macromolecules* **1992**, *25*, 2603.
(2) Dias, A. J.; McCarthy, T. J. *Macromolecules* **1987**, *20*, 2819.
(3) Dias, A. J.; McCarthy, T. J. *Macromolecules* **1987**, *20*, 2819.
(4) Lee, K.-W.; McCarthy, T. J. *Macromolecules* **1988**, *21*, 3353.
(5) Bee, T. G.; McCarthy, T. J. *Macromolecules* **1992**, *25*, 2093.
(6) Dias, A. J.; McCarthy, T. J. *Macromolecules* **1984**, *17*, 2529.
(7) Lee, K.-W.; McCarthy, T. J. *Macromolecules* **1988**, *21*, 309.
(8) Bening, R. C.; McCarthy, T. J. *Macromolecules* **1990**, *23*, 2648.
(9) Franchina, N. L.; McCarthy, T. J. *Macromolecules* **1991**, *24*, 3045.
(10) Koros, W. J.; Fleming, G. K *J. Membr. Sci.* **1993**, *83*, 1.
(11) Mohr, J. M.; Paul, D. R.; Pinnau, I.; Koros, W. J. *J. Membr. Sci.* **1991**, *56*, 77.
(12) Chiao, C. C. U.S. Patent 4,828,585, 1989.
(13) Mohr, J. M.; Paul, D. R.; Mlsna, T. E.; Lagow, R. J. *J. Membr. Sci.* **1991**, *55*, 131.
(14) Puleo, A. C.; Paul, D. R. *Polymer* **1989**, *30*, 1357.

MA941307J